Copper (II) Oxide Nanowires for p-type Conductometric NH_3 Sensing

F.Shao[1], F.Hernández-Ramírez[1,2*], J.D. Prades[2], C.Fàbrega[1], T. Andreu[1], J.R.Morante[1,2]

[1] *Catalonia Institute for Energy Research (IREC), C. Jardins de les Dones de Negre 1, 08930 Sant Adrià del Besòs, Spain*

[2] *Department of Electronics, University of Barcelona, C. Marti i Franqués 1, 08028 Barcelona, Spain*

* Author to whom correspondence should be addressed: fhernandez@irec.cat

Tel: +34 933 562 615; Fax: +34 933 563 802

Abstract

Copper (II) oxide (CuO) is a metal oxide suitable for developing solid state gas sensors. Nevertheless, a detailed insight into the chemical-to-electrical transduction mechanisms between gas molecules and this metal oxide is still limited. Here, individual CuO nanowires were evaluated as ammonia (NH_3) and hydrogen sulphide (H_2S) sensors, validating the p-type character of this semiconductor. The working principle behind their performance was qualitatively modelled and it was concluded that adsorbed oxygen at the surface plays a key role necessary to explain the experimental data. Compared to their counterparts of SnO_2 nanowires, an appreciable sensitivity enhancement to NH_3 for concentrations below 100 ppm was demonstrated.

Key words: CuO, nanowire, gas sensor, semiconductor

1. Introduction

Metal oxides (MOX) show outstanding sensing properties to different chemical species with simple and cost effective device configurations [1-3]. Compared to n-type metal oxides, the existing knowledge about the surface chemistry of gas molecules onto p-type materials remains however poorly explored.

Also known as cupric oxide, copper (II) oxide (CuO) is a p-type metal oxide with a bandgap of about 1.4 eV, suitable for electrochemical cells, photovoltaic, field emission and gas sensing devices [4-6]. In this latter application, films of CuO were reported to detect O_3, CO and C_5H_2OH among other chemical species [7-9]. Recently, the potential of CuO nanowires as building-blocks of new devices has been pointed out [10-14]. Among the different techniques to synthesize CuO nanowires, such as electro-spinning [17] and template-assisted growth [11], the direct oxidation of Cu foils [14-16] is easy to implement and scalable, providing pleasing results in terms of crystallinity and material quality [14]. These facts are triggering the research on one-dimensional (1D) CuO nanostructures [5, 12, 13, 15, 16], but the scope of their sensing characteristics remains uncompleted according to the authors' best knowledge since the studies performed with individual CuO nanowires have been limited up to now [12, 13, 15].

It is the aim of this work to shed some light on the sensor potential of CuO nanowires, because the comprehension of the surface chemistry of pollutants in MOX is crucial to improve the performance of future devices. Here, we prepared CuO nanowires by thermal oxidation and electrical characterizations were made to individual devices contacted in 4-probe configuration. Responses to NH_3 and H_2S of the nanowires were examined to qualitatively describe the working principle behind their performance, paving the way to more complex studies that combine experimental data and simulation studies in the same way that previous works on SnO_2 nanowire sensors [17]. Here, an unequivocal correlation was established between the experimental data and the p-character of the

CuO. Besides, all nanowires showed stable and reproducible responses to these chemical species. Comparing to the response of sensors made from n-type SnO_2 nanowires, a higher sensitivity to NH_3 was demonstrated for CuO.

2. Material and Methods

CuO nanowires were prepared by heating in open-air atmosphere high purity (99.9%) copper foils of thickness 0.25 mm. To remove the native oxide, the foils were firstly soaked in 1.5 M HCl for 10 min and then rinsed with deionized water and acetone. Later, they were dried with compressed N_2 flux. The furnace was pre-heated to 500ºC before placing the Cu foils in. Growth times were changed from 0.5 to 8 hours to evaluate the influence of this parameter in the final morphology of the samples. After reaching the required time, the samples were allowed to cool down by themselves. The crystallographyic phases of the CuO were examined by X-ray diffraction (XRD) using a Bruker D8 Advance diffractometer with Cu Kα radiation. Morphology of the nanowires was observed using a Zeiss (Auriga) scanning electron microscope (SEM) equipped with an Oxford X-ray energy dispersive spectrometer for EDS analysis. Monocrystalline SnO_2 nanowires were synthesized by chemical vapor deposition (CVD) following a process described elsewhere [18].

Electrical measurements were performed on two individual CuO nanowires contacted by Pt nanoelectrodes on Si/SiO_2 substrates deposited by means of combined focused ion beam and electron beam (FIB/EB) assisted lithography, following a process described earlier [19]. To that end, the 4-probe configuration was preferred to avoid contact resistance effects.

Two-probe devices were tested as gas sensors inside an air tight chamber (LTS350, Linkam) especially designed to minimize the external noise. Annealing of as deposited Pt contacts was performed at 300ºC for 2 h. Heating of the nanowire was realized with the in-built heater of the chamber and the measurements were made with a Sourcemeter (2635A, Keithley). Gas mixtures were precisely produced with thermal mass-flow controllers and certified gas bottles, with a constant

total gas flow rate of 200 sccm. The working temperature was always below 300ºC to avoid damaging the FIB/EB contacts [20, 21]

To take into account the p-type character of CuO nanowires, the sensitivity *S* was defined as,

$$S = R_{gas} / R_{SA} \quad (1)$$

where R_{gas} is the device resistance after exposure to the target gases, and R_{SA} is the resistance in synthetic air. On the contrary, *S* of n-type SnO_2 nanowires [17] was calculated as,

$$S = R_{SA} / R_{gas} \quad (2)$$

The response/recovery time (τ_r/τ_{rec}) was defined as the necessary time to complete 90% of the resistance changes.

3. Results and Discussion

After the thermal oxidation, Cu foils were covered by an easy detachable black layer where CuO nanowires were located on its surface. The growth was found to be more profound in the first 2 h as no clear increase in the nanowire length was observed in the longer heated samples. In addition, we observed the inhomogeneous of length inside each sample. The nanowires usually grew into two typical length ranges: roughly 3 to 5 μm and 10 to 15 μm for the 1 h growth; 5 to 10 μm and 15 to 25 μm for the longer growth times. Fig. 1 shows top and side view of CuO nanowires after 1 and 8 h of thermal oxidation. SEM images of other growth time can be found in the support information.

XRD pattern in Fig.2 shows the coexistence of Cu_2O and CuO phases in the processed samples. Cu peaks were not observable since the metal was completely covered by the oxide layers. Selected Area EDS (SAEDS) analysis on the cross-section of the oxidized layers gave a Cu/O atomic ratio of roughly 1.8 at the bottom part and 0.8 at the interface/nanowire part (Fig.3). Considering the

accuracy limit of EDS technique and the potential interfering effect of adsorbed molecules, e.g., H_2O and O_2, it was concluded that Cu_2O and CuO were formed at the bottom and top of the oxidized section, respectively. In fact, the three phases (Cu, Cu_2O and CuO) can coexist at temperatures below 1050ºC [22]. The nanowires were formed by the progressive oxidation of the copper substrate as follows,

$$4Cu + O_2 \leftrightarrow 2Cu_2O \quad (3)$$

$$2Cu_2O + O_2 \leftrightarrow 4CuO \quad (4)$$

Thus, the final relative amount of Cu_2O and CuO in the samples strongly depends on the temperature and the oxygen partial pressure during the thermal annealing.

4-probe electrical measurements on an individual nanowire of about 20.7 μm long and 100 nm in diameter (Fig.4) revealed a conductivity (σ) of $6.9\times10^{-3}\ \Omega^{-1}cm^{-1}$, which is on the same order of magnitude as values obtained previously with CuO nanowires operated in FET configuration ($1.1\times10^{-3}\ \Omega^{-1}cm^{-1}$) [12], and sputtered CuO thin films ($5.6\times10^{-3}\ \Omega^{-1}cm^{-1}$) [23]. Here, the geometry of the nanowire was estimated by direct SEM observation (see Fig.S2 in support information). The relative larger conductivity of our devices is ascribable to the exclusion of contact resistance contribution in this measurement geometry and the eventual Pt deposition near the contact-nanowire junctions in the FIB/EB processing [19, 24].

The sensing characteristics of individual CuO nanowires were evaluated after the exposure of some devices to NH_3 diluted in dry synthetic air (SA). For the sake of simplicity, humidity effects were not considered in this work. Competing interactions in the presence of moisture complicate the effective modeling of the MOX surface chemistry [17].

The typical performance of a CuO nanowire with diameter of about 200 nm (see Fig.S3 in support information) is depicted in Fig.5. For NH_3 sensing, the optimal working conditions were observed at

around 200ºC. At this temperature, *S* reached values up to 3.1 without evidence of signal saturation at the highest gas concentration, $[NH_3]$ = 100 ppm. Response time τ_r was estimated to be about 6 minutes and longer recovery times (τ_{rec} ~ 30 min) were found in all cases (Fig.5a). Lower temperatures lead to high resistance values that made difficult the gas tests. The sensing mechanism of NH_3 by CuO was explored in the past [15, 25]. To that end, the classic conduction model [26] of metal-oxides was adopted; surface oxygen species withdraw electrons from CuO decreasing the resistance due to the generation of holes in the material. Upon exposure to NH_3, the reaction path at the CuO surface can be given as follows,

$$O_2^-/O^-/O^{2-} + NH_3\ (ad) \leftrightarrow N_{species} + H_2O + e^- \quad (5)$$

Actually, NH_3-CuO interactions are complex and they may involve reaction paths with different charge exchanges such as [27],

$$3O_2^- + 4NH_3 \leftrightarrow 2N_2 + 6H_2O + 3e^- \quad (6)$$

$$3O^- + 2NH_3 \leftrightarrow N_2 + 3H_2O + 3e^- \quad (7)$$

$$3O^{2-} + 2NH_3 \leftrightarrow N_2 + 3H_2O + 6e^- \quad (8)$$

In short, adsorbed ammonia molecules and surface oxygen species react, with N_2 and H_2O as the main resulting products. Released electrons then diminish hole concentration in the nanowire thereby the resistance of the material finally increases in agreement with the experimental data (Fig.5), backing up the p-type character of CuO.

S in MOX is usually expressed as a power law of the concentration of the target gas $[C]$ where β denotes a constant:

$$S \sim \beta[C]^{\alpha} \quad (9)$$

Previous works on individual SnO_2 nanowires demonstrated that the relationship given in eq.9 is followed by very similar device configurations and gas measurements [33]. In practise, α is a parameter dependent on the experimental conditions and the intrinsic properties of the metal oxide, such as the material quality and the diameter in the case of nanowires [28-30]. From the validity of this model in individual nanowires three conclusions are implied [26, 33]: (i) the resistance change induced by the analyte is ascribable to the width modulation of the conduction channel due to the formation of a depleted region beside the surface, (ii) the ionosorbed oxygen at the metal oxide plays a key role in the sensing mechanism, and (iii) the concentration of the tested analyte is significant lower that the total oxygen species at the surface. Three devices followed the power law reported in eq.9 (inset of Fig.5a), with the exponent close to $\alpha \approx 0.4$. Yamazoe et al. [28] reported that α takes different values in porous films depending on the morphology of the sample and size of the nanoparticles among other parameters [30,31]. In our case, the α value is higher than the obtained with individual SnO_2 nanowires with diameter about 100 nm obtained following an equivalent procedure ($\alpha \approx 0.07$) [17]. SnO_2 devices fabricated with alternative methodologies showed different α values highlighting the strong influence in this parameter of changes in the device processing [33].

Our CuO nanowires ($S = 3.1$) showed also a higher sensitivity than SnO_2 ($S = 1.5$) to $[NH_3] = 100$ ppm, which results in a significant advantage for NH_3 detection. The difference observed in these two parameters (α, S) as well as the dissimilar behaviour of the sensitivity as function of the temperature (Fig.5b) are a direct proof that the surface chemistry is significantly different in the two metal oxides, since the response modulation as function of the diameter is considered a second order effect in this diameter range (d > 100 nm) [31]. Actually, the bell-shaped form of the response with increasing surface temperature in MOX was explained by Ahlers et al. [32] in terms of two competing surface processes and as a consequence the experimental curve for SnO_2 and CuO nanowires can be parameterised by means of two energetic parameters: the strength of Langmuir adsorption E_{ads} of the NH_3 molecule at the surface, and the activation energy for the combustion reaction E_{RES}. These two

factors are thus the decisive parameters to explain the high-temperature drop-off of *S*. Despite the complete description of the NH_3-CuO interaction mechanism is beyond the scope of this preliminary work, it can be concluded from the dissimilar response-to-temperature profile and assuming that E_{ads} is comparable in both metal oxides that the activation energy E_{RES} is larger for SnO_2 .

To evaluate the overall performance of our devices upon exposure to other reducing species, H_2S sensing (< 10 ppm) was also done at different working temperatures. In the same way that NH_3 detection, stable and reproducible response were always observed with this later gas (Fig.6a). Clearly, the interaction mechanism of H_2S and CuO was a thermally activated process with the maximum response at 300ºC (Fig.6a). Experiments at higher temperatures were not performed to avoid the damage of the Pt contacts thereby the optimal point for H_2S sensing could not be determined. At 300ºC, pulses from 500 ppb to 10 ppm were detected without evidence of signal saturation at the highest concentration. Again, the sensing mechanism of this reducing gas was explained by the interaction with the oxygen species at the CuO surface. Water and sulphur dioxide were identified as the main resulting products [7],

$$O_2^-/O^-/O^{2-} + H_2S\ (ad) \leftrightarrow H_2O + SO_2 + e^- \qquad (10)$$

Consequently, released electrons lead to a resistance rise of CuO upon exposure to H_2S atmosphere due to the p-type character of this MOX. Similarly to the NH_3 case, it should be pointed out that eq.10 is a simplification of a more complex sensing process.

It is well-known that in parallel CuO can go through a sulphurisation process resulting in a huge drop of the resistance due to the formation of metallic CuS at the surface. This mechanism is expected to occur at high H_2S concentrations [8, 14] and in our case it was not experimentally observed. Therefore, it should be considered a second order effect at most.

Now, the performance of CuO nanowires as H_2S sensors was comparable to that found in SnO_2 devices (Fig. 6b); responses were observed with $\alpha \approx 0.1$ for both materials. On the other hand, the

continuous increase of S (Fig. 6b) with temperature by CuO indicates that E_{RES} is much larger in CuO devices.

From these findings, it is concluded that CuO nanowires are p-type semiconductors that suit well for sensing applications. The analysis of their responses to NH_3 and H_2S suggests that the chemical-to-electrical transduction mechanisms between gas molecules and CuO are clearly dominated by adsorbed oxygen at the metal oxide surface. Compared to sensors based on SnO_2 nanowires, an appreciable sensitivity enhancement to NH_3 was demonstrated, unveiling an intrinsic advantage of using CuO nanowires for this particular application in the diameter range between 100 nm and 200 nm.

4. Conclusions

CuO nanowires were synthesized and evaluated as gas sensors. The electrical conductivity was determined and the devices exhibited stable and reproducible responses towards the gas pollutants. The analysis of the responses to NH_3 and H_2S demonstrated the p-type character of this metal oxide while adsorbed oxygen at the surface is crucial to model experimental responses. In particular, promising results as NH_3 sensors were found with higher sensitivity values than those obtained with SnO_2 nanowires.

Acknowledgments

The research was supported by the Framework 7 program under the project S3 (FP7-NMP-2009-247768) and European Regional Development Funds (ERDF) “FEDER Programa Competitivitat de Catalunya 2007–2013”).

References

[1] G. Korotcenkov, Metal Oxides for Solid-state Gas Sensors: What Determines our Choice?, Mater. Sci. Eng. B 139 (2007) 1–23.

[2] C. Baratto, E. Comini, G. Faglia, G. Sberveglieri, M. Zha, A. Zappettini, Metal oxide nanocrystals for gas sensing, Sensors and actuators B, 109 (2005) 2–6.

[3] J. Huang, Q. Wan, Gas Sensors Based on Semiconducting Metal Oxide One-dimensional Nanostructures, Sensors, 9 (2009) 9903–9924.

[4] A. Gurbani, J.L. Ayastuy, M.P. González-Marcos, M.A. Gutiérrez-Ortiz, CuO–CeO_2 catalysts synthesized by various methods: Comparative study of redox properties, International Journal of Hydrogen Energy, 35 (2010) 11582-11590.

[5] P. Shao, S. Deng, J. Chen, J. Chen, N. Xu, Study of field emission, electrical transport, and their correlation of individual single CuO nanowires, Journal of Applied Physics, 109 (2011) 023710-023716.

[6] B.K. Meyer, A. Polity, D. Reppin, M. Becker, P. Hering, P.J. Klar, T. Sander, C. Reindl, J. Benz, M. Eickhoff, C. Heiliger, M. Heinemann, J. Bläsing, A. Krost, S. Shokovets, C. Müller, C. Ronning, Binary copper oxide semiconductors: From materials towards devices, physica status solidi (b), 249 (2012) 1487-1509.

[7] F. Zhang, A. Zhu, Y. Luo, Y. Tian, J. Yang, Y. Qin, CuO Nanosheets for Sensitive and Selective Determination of H_2S with High Recovery Ability, The Journal of Physical Chemistry C, 114 (2010) 19214-19219.

[8] N.S. Ramgir, S.K. Ganapathi, M. Kaur, N. Datta, K.P. Muthe, D.K. Aswal, S.K. Gupta, J.V. Yakhmi, Sub-ppm H_2S sensing at room temperature using CuO thin films, Sensors and Actuators B: Chemical, 151 (2010) 90-96.

[9] M. Hübner, C.E. Simion, A. Tomescu-Stănoiu, S. Pokhrel, N. Bârsan, U. Weimar, Influence of humidity on CO sensing with p-type CuO thick film gas sensors, Sensors and Actuators B: Chemical, 153 (2011) 347-353.

[10] J. Chen, K. Wang, L. Hartman, W. Zhou, H_2S Detection by Vertically Aligned CuO Nanowire Array Sensors, J. Phys. Chem. C, 112 (2008) 16017- 16021.

[11] X. Li, Y. Wang, Y. Lei, Z. Gu, Highly sensitive H_2S sensor based on template-synthesized CuO nanowires, RSC Advances, 2 (2012) 2302-2307.

[12] D.D. Li, J. Hu, R.Q. Wu, J.G. Lu, Conductometric Chemical Sensor based on Individual CuO Nanowires, Nanotechnology, 21 (2010) 485502.

[13] L. Liao, Z. Zhang, B. Yan, Z. Zheng, Q.L. Bao, T. Wu, C.M. Li, Z.X. Shen, J.X. Zhang, H. Gong, J.C. Li, T. Yu, Multifunctional CuO nanowire devices: p-type field effect transistors and CO gas sensors, Nanotechnology, 20 (2009) 085203.

[14] D. Zappa, E. Comini, R. Zamani, J. Arbiol, J.R. Morante, G. Sberveglieri, Preparation of copper oxide nanowire-based conductometric chemical sensors, Sensors and Actuators B: Chemical, 182 (2013) 7-15.

[15] B.J. Hansen, N. Kouklin, G. Lu, I.K. Lin, J. Chen, X. Zhang, Transport, Analyte Detection, and Opto-Electronic Response of p-Type CuO Nanowires, The Journal of Physical Chemistry C, 114 (2010) 2440-2447.

[16] C.Y. Huang, A. Chatterjee, S.B. Liu, S.Y. Wu, C.L. Cheng, Photoluminescence properties of a single tapered CuO nanowire, Applied surface science, 256 (2010) 3688-3692.

[17] F. Shao, M.W.G. Hoffmann, J.D. Prades, J.R. Morante, N. López, F. Hernández-Ramírez, Interaction Mechanisms of Ammonia and Tin Oxide: A Combined Analysis Using Single Nanowire Devices and DFT Calculations, The Journal of Physical Chemistry C, 117 (2013) 3520-3526.

[18] S. Mathur, S. Barth, H. Shen, J.-C. Pyun, U. Werner, Size-dependent Photoconductance in SnO_2 Nanowires, small, 1 (2005) 713–717.

[19] F.H. Ramirez, A. Tarancon, O. Casals, J. Rodriguez, A. Romano-Rodriguez, J.R. Morante, S. Barth, S. Mathur, Y. Choi T, D. Poulikakos, V. Callegari, P.M. Nellen, Fabrication and Electrical Characterization of Circuits based on Individual Tin Oxide Nanowires, Nanotechnology, 17 (2006) 5577–5583.

[20] F. Hernandez-Ramirez, A. Tarancon, O. Casals, E. Pellicer, J. Rodriguez, A. Romano-Rodriguez, J.R. Morante, S. Barth, S. Mathur, Electrical properties of individual tin oxide nanowires contacted to platinum electrodes, Physical Review B, 76 (2007) 085429.

[21] J.D. Prades, R. Jimenez-Diaz, F. Hernandez-Ramirez, S. Barth, A. Cirera, A. Romano-Rodriguez, S. Mathur, J.R. Morante, Ultralow Power Consumption Gas Sensors Based on Self-heated Individual Nanowires, Appl. Phys. Lett., 93 (2008) 123110.

[22] ASM Handbook Volume 03: Alloy Phase Diagrams, ASM International, 1992.
[23] A. Parretta, M.K. Jayaraj, A. Di Nocera, S. Loreti, L. Quercia, A. Agati, Electrical and Optical Properties of Copper Oxide Films Prepared by Reactive RF Magnetron Sputtering, physica status solidi (a), 155 (1996) 399-404.
[24] R. Steve, P. Robert, A review of focused ion beam applications in microsystem technology, Journal of Micromechanics and Microengineering, 11 (2001) 287.
[25] R.K. Bedi, I. Singh, Room-Temperature Ammonia Sensor Based on Cationic Surfactant-Assisted Nanocrystalline CuO, ACS Applied Materials & Interfaces, 2 (2010) 1361-1368.
[26] N. Barsan, U. Weimar, Conduction Model of Metal Oxide Gas Sensors, J. Electroceram., 7 (2001) 143−167.
[27] N.V. Hieu, V.V. Quang, N.D. Hoa, D. Kim, Preparing Large-scale WO_3 Nanowire like Structure for High Sensitivity NH_3 Gas Sensor Through a Simple Route, Curr. Appl. Phys., 11 (2011) 657−661.
[28] N. Yamazoe, K. Shimanoe, Theory of power laws for semiconductor gas sensors, Sensors and Actuators B: Chemical, 128 (2008) 566-573.
[29] L.V. Thong, L.T.N. Loan, N. Van Hieu, Comparative study of gas sensor performance of SnO2 nanowires and their hierarchical nanostructures, Sensors and Actuators B: Chemical, 150 (2010) 112-119.
[30] Y.J. Chen, X.Y. Xue, Y.G. Wang, T.H. Wang, Synthesis and ethanol sensing characteristics of single crystalline SnO2 nanorods, Applied Physics Letters, 87 (2005) -.
[31] F. Hernandez-Ramirez, J.D. Prades, A. Tarancon, S. Barth, O. Casals, R. Jimenez-Diaz, E. Pellicer, J. Rodriguez, J.R. Morante, M.A. Juli, S. Mathur, A. Romano-Rodriguez, Insight into the Role of Oxygen Diffusion in the Sensing Mechanisms of SnO2 Nanowires, Advanced Functional Materials, 18 (2008) 2990-2994.
[32] S. Ahlers, G. Müller, T. Doll, A rate equation approach to the gas sensitivity of thin film metal oxide materials, Sensors and Actuators B: Chemical, 107 (2005) 587-599.

[33]D.C. Meier, S. Semancik, B. Button, E. Strelcov, A. Kolmakov, Coupling nanowire chemiresistors with MEMS microhotplate gas sensing platforms, Applied Physics Letters, 91 (2007) 063118.

Figure Captions

Fig. 1. Top and side view of CuO nanowires grown after 1 h (1a & 1b) and 8 h (2a & 2b) of thermal oxidation. Scale bars are 1 μm for top view and 10 μm for side view.

Fig. 2. XRD pattern of a copper film after thermal oxidation for 4 h at 500ºC in air. (Inset) Cross-sectional diagram of the as-formed phases in the foil.

Fig. 3. Cross-sectional SEM image of the oxide layer on Cu foil. Cu_2O was found in the bottom layer while CuO nanowires are visible on the top (the composition data are given by the SAEDS analysis).

Fig. 4. 4-probe I-V curve obtained with a CuO nanowire at room temperature. (Inset) SEM image of a device made up of a single CuO nanowire, scale bar is 2 μm.

Fig. 5. (a) Dynamic response exhibited by a CuO nanowire at a working temperature of 200ºC towards a sequence of NH_3 pulses of different concentrations. (Inset) Sensitivity as function of NH_3 concentration. (b) Sensitivity of a CuO nanowire and a SnO_2 nanowire towards 50 ppm of NH_3 as function of the temperature. Higher values are observed for CuO while a dissimilar behavior is clearly found. Dashed line qualitatively represent the region where the activation energy for the combustion reaction E_{RES} determines the sensor response.

Fig. 6. (a) Dynamic response exhibited by a CuO nanowire at a working temperature of 300ºC towards a sequence of H_2S pulses of different concentrations. (Inset) Sensitivity as function of H_2S concentration. (b) Sensitivity of a CuO and SnO_2 nanowire to 10 ppm of H_2S as function of the temperature.

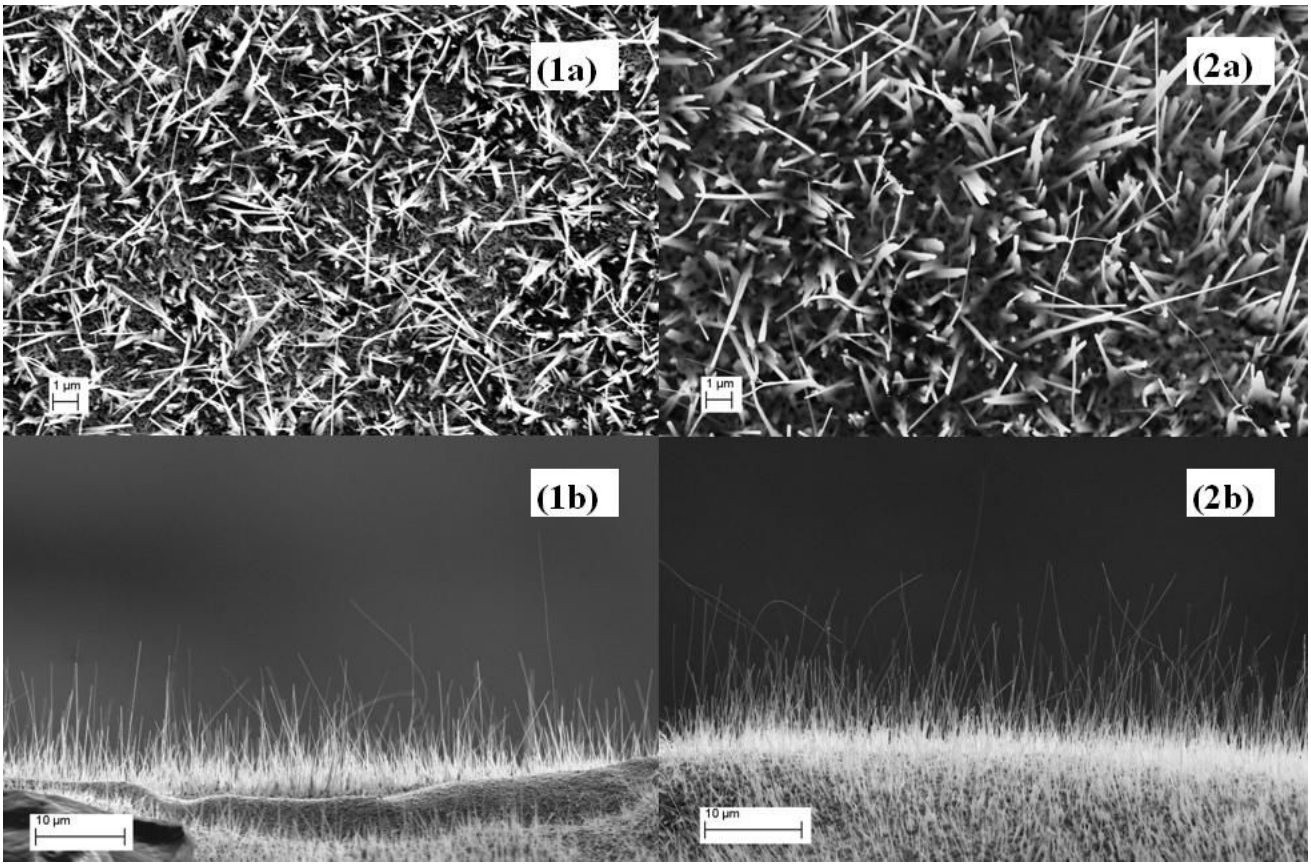

Fig. 1. Top and side view of CuO nanowires grown after 1 h (1a & 1b) and 8 h (2a & 2b) of thermal oxidation. Scale bars are 1 µm for top view and 10 µm for side view.

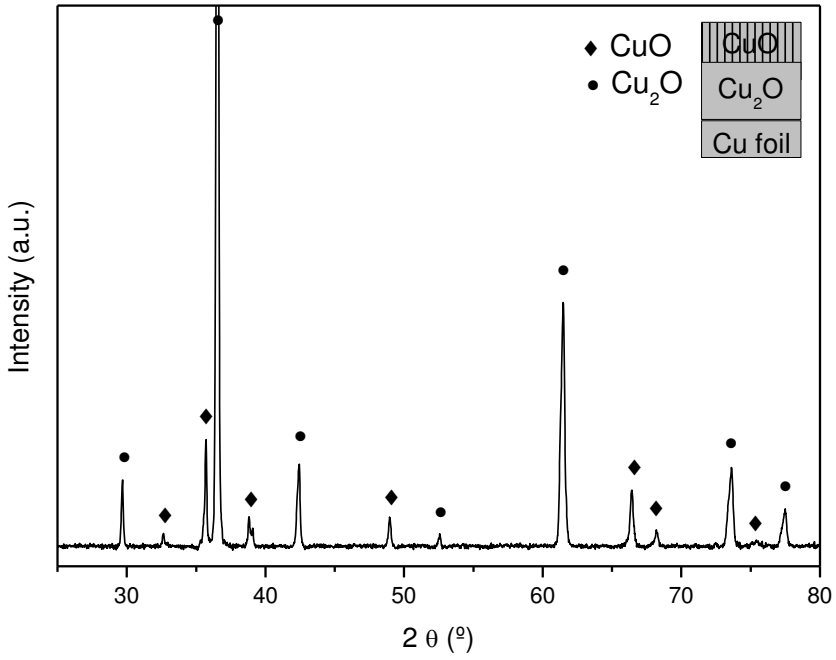

Fig. 2. XRD pattern of a copper film after thermal oxidation for 4 h at 500ºC in air. (Inset) cross-sectional diagram of the as-formed phases in the foil.

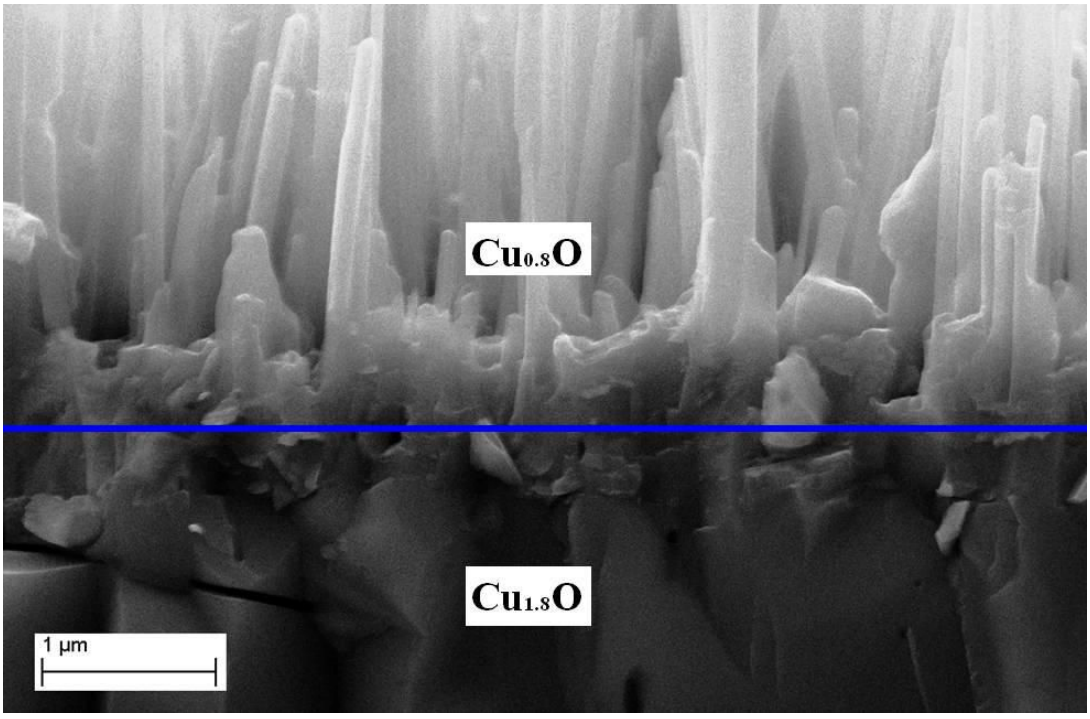

Fig. 3. Cross-sectional SEM image of the oxide layer on Cu foil. Cu_2O was found in the bottom layer while CuO nanowires are visible on the top (the composition data are given by the SAEDS analysis).

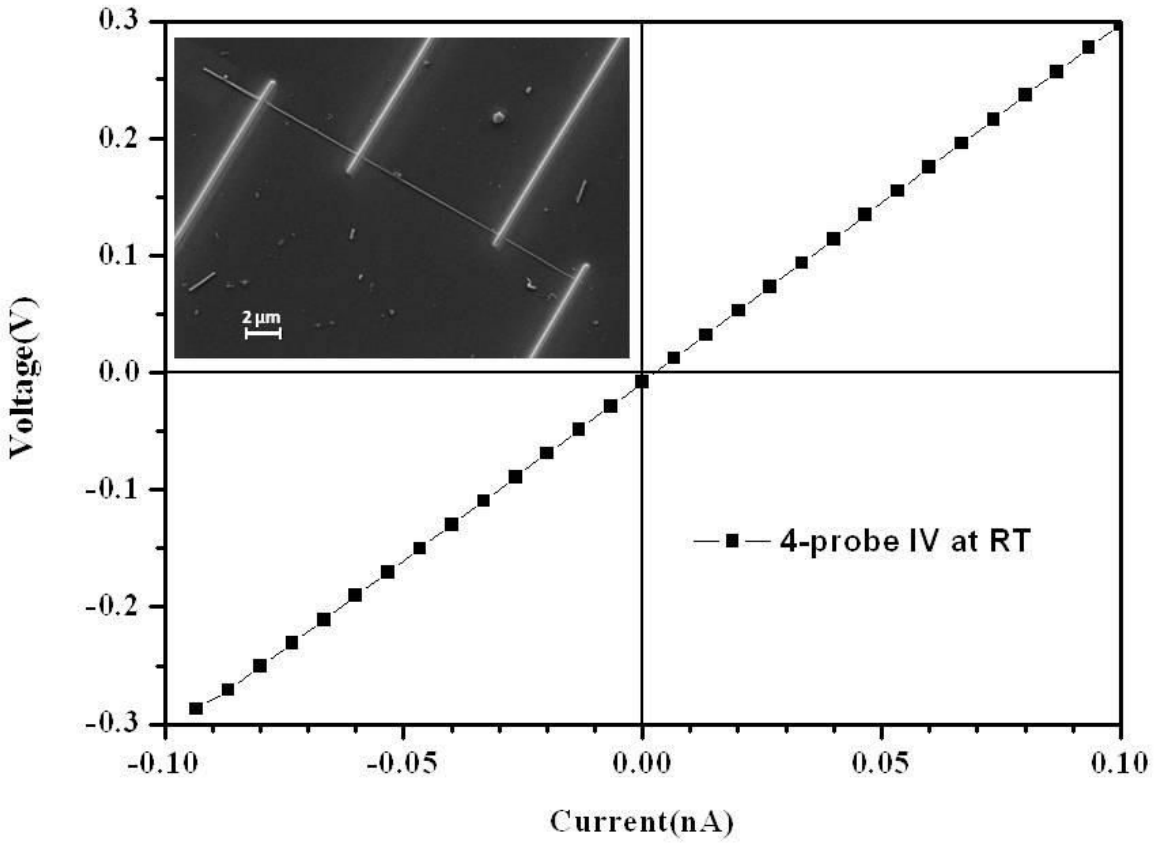

Fig. 4. 4-probe I-V curve obtained with a CuO nanowire at room temperature. (Inset) SEM image of a device made up of a single CuO nanowire, scale bar is 2 μm.

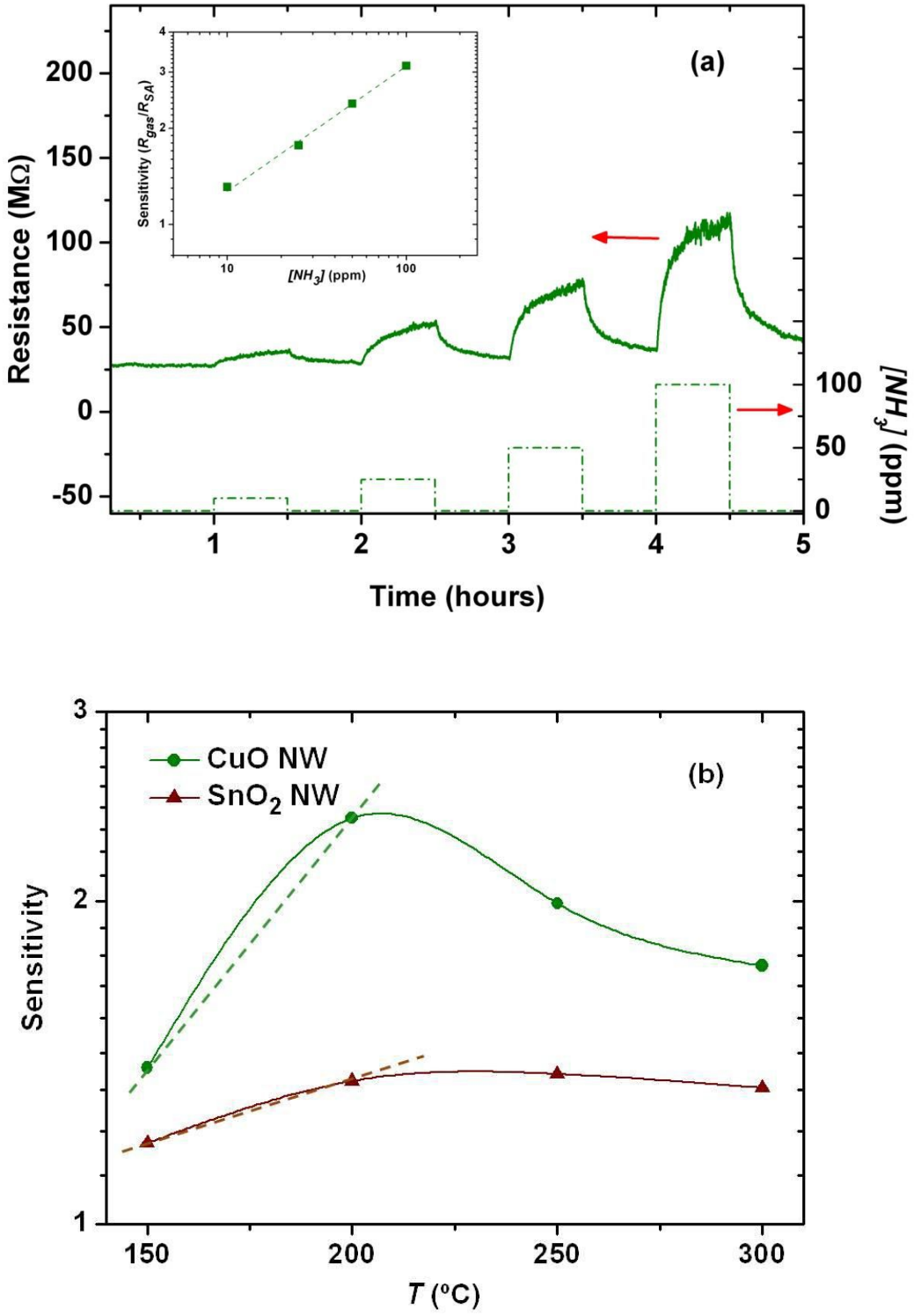

Fig. 5. (a) Dynamic response exhibited by a CuO nanowire at a working temperature of 200ºC towards a sequence of NH_3 pulses of different concentrations. (Inset) Sensitivity as function of NH_3 concentration in log-log scale. (b) Sensitivity of a CuO nanowire and a SnO_2 nanowire towards 50 ppm of NH_3 as function of the temperature. Higher values are observed for CuO while a dissimilar behavior is clearly found. Dashed line qualitatively represent the region where the activation energy for the combustion reaction E_{RES} determines the sensor response.

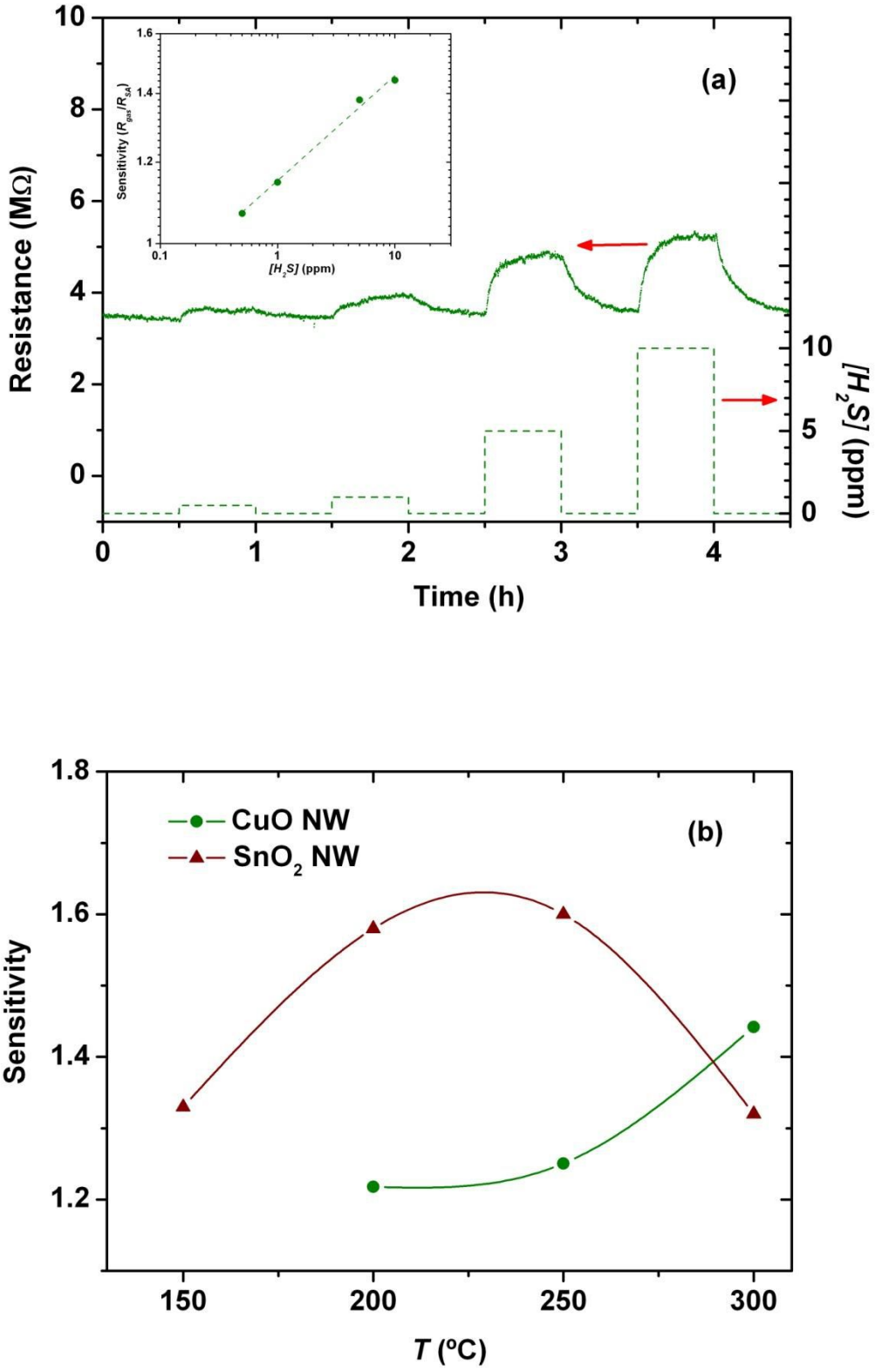

Fig. 6. (a) Dynamic response exhibited by a CuO nanowire at a working temperature of 300ºC towards a sequence of H_2S pulses of different concentrations. (Inset) Sensitivity as function of H_2S concentration in log-log scale. (b) Sensitivity of a CuO and SnO_2 nanowire to 10 ppm of H_2S as function of the temperature.